Control-Augmented Structural Synthesis with Dynamic Stability Constraints

H. L. Thomas* and L. A. Schmit Jr.†
University of California, Los Angeles, Los Angeles, California 90024

Dynamic stability constraints are included in a computer program that simultaneously synthesizes a structure and its control system. Two measures of stability – the real part of the system complex eigenvalues and the damping ratio – are examined. The procedure for calculating the sensitivities of the two measures of stability to changes in the structure and its control system is explained. The sensitivities are used to formulate an approximate optimization problem that is solved at each design iteration. The effects of structural damping and noncollocated controllers on the synthesis process are discussed.

Introduction

LARGE space structures, which will be very flexible due to low weight requirements, will need some type of active control system to suppress vibration and to maintain stringent shape specifications.[1,2] Vibrations and shape variations can be induced by positioning maneuvers, motion of mass within the structure, thermal gradients, and docking procedures. Stringent shape specifications are required to maintain pointing accuracy of optical and radar equipment. Because of their size and flexibility, large space structures will have vibrations with low frequencies and long decay times. Because of the low frequencies of vibration, the structural and control system dynamics may interact. This work is an extension of the control-augmented structural synthesis capability reported in Refs. 3 and 4 to include noncollocated controllers and dynamic stability constraints. A description of a general controller and the stability constraints is given. Numerical examples are presented to show the effect of the stability constraints on the design optimization.

Background

The usual approach to structure-control system synthesis is first to design the structure, with constraints on weight, static and dynamic displacements and stresses, and open-loop eigenvalues (natural frequencies), and then to design a control system for this structure, with constraints on the closed-loop eigenvalues (poles), dynamic response, and control force. If the constraints on the control system design cannot be met, the structure is redesigned and another pass is made at the control system design. Typically this iterative cycling occurs because the structure is designed for low weight and therefore, is very flexible. Because of this flexibility, excessive control force is needed. Changes in the structural design can also lead to beneficial changes in the closed-loop eigenvalues, especially if some type of inherent or passive structural damping is present. Structural modifications also lead to changes in the control system, especially if linear optimal control theory is used for the control system design. Because of the iterative nature of this approach to structure-control system design, with two sets of objective functions and constraints, convergence to a final design may be slow. Simultaneous synthesis of the structure-control system overcomes the problem of the sequential iterative approach because there is one set of constraints and the interaction of structural and control system dynamics is taken into account.

There are three main approaches taken to the simultaneous structure-control system design problem. The difference between these approaches is in how the control system gains and forces are determined. In the first approach, an objective function that is a weighted sum of the structural mass and the control system quadratic performance index is minimized for a structure-control system that is subjected to a specified transient load or that must complete a transient maneuver in a specified finite time.[5,6] The solution to this problem involves numerically integrating a system of coupled nonlinear equations to find the optimal structure and control system forces. These control forces are then applied to the structure in an open-loop manner. The drawback to this approach is that specific response constraints cannot be easily applied to the structure or the control system.

In the second approach, the control system gain design variables are dependent on the structural design variables, and they are determined by the solution of the Riccati equation. This is the approach taken in Refs. 7–15. In Refs. 7–13, the objective function is the structural mass and/or quadratic performance index. Constraints are placed on open- and closed-loop eigenvalues and/or structural mass. In Refs. 11–13, the performance index is not included in the objective function, and therefore the optimization process does not try to change the structural variables to lower the performance index. It should also be noted that the calculation of sensitivities of the closed-loop eigenvalues with respect to the structural design variables, which are needed for efficient optimization, is quite costly since the Riccati equation must be solved many times. This is because of the dependent nature of the control system gains. Also in Refs. 7–13, no external loads are applied so no actual displacements or forces are constrained or minimized. In Ref. 14, the performance index and mass are minimized sequentially for a structure undergoing a transient rest-to-rest maneuver. In Ref. 15, the objective function is an unknown but bounded disturbance to be maximized with constraints on displacements and actuator forces.

In the first two approaches, the quadratic performance index is minimized. This expression contains two weighting matrices that must be specified by the user. A different "optimal" design will be generated with different weighting matrices. The components of these weighting matrices can even be used as design variables.[12,13] The matrices cannot be generated so that the structure-control system will meet force and displacement constraints under external applied loads without some a priori knowledge of the final design. One practical approach is to

Presented as Paper 89-1216 at the AIAA/ASME/ASCE/AHS/ASC 30th Structures, Structural Dynamics, and Materials Conference, Mobile, AL, April 3–5, 1989; received Oct. 4, 1989; revision received March 29, 1990.

*Graduate Research Assistant; currently, Research Engineer, VMA Engineering, 5960 Mandarin Ave., Suite F, Goleta, CA 93317. Member AIAA.

†Professor of Engineering and Applied Science. Fellow AIAA.

form the weighting matrices so that the performance index represents the total energy of the system (see for example Ref. 9).

The third approach to structure-control system synthesis is truly integrated because structural design variables and control gains are simultaneously treated as independent design variables.[15-20] In Ref. 15, a bounded but unknown input force is maximized with constraints on displacements and actuator forces. In Refs. 16–18, the objective function to be minimized is the sum of the gains or norm of the gain matrix. Constraints are placed on open- and/or closed-loop eigenvalues. This choice of objective function is convenient but not practical as low gains do not necessarily lead to low control forces. In Ref. 19, the structural mass is minimized, and constraints are placed on the closed-loop eigenvalues. There are no constraints on structural responses in this work. In Ref. 20, a weighted sum of the structural mass and control force is minimized with constraints on displacements and the real part of the closed-loop eigenvalues for a structure subjected to a distributed white noise force.

In the work reported here, the third approach is adopted and both structural sizing and control system gains are treated as strictly independent design variables. Two alternative objective functions are considered, namely minimization of mass or minimization of total control force. The mix of response measures that can be constrained includes closed-loop eigenvalues and damping ratios, harmonic dynamic displacements and rotations, controller forces, and undamped natural frequencies. Upper limits on total control force and/or structural mass can also be imposed. The integral structure-control system design optimization problem is formulated as a nonlinear programming problem in a design space that spans the structural sizing variables as well as the control system gains, and all of the constraints are treated simultaneously.

Noncollocated Control System

It is desirable to have the option to use noncollocated sensor-actuator pairs because it gives the control system designer more flexibility. Noncollocation may often have to be used because of physical placement or hardware limitations. It may be necessary to place a sensor in a location that gives good data but is not a feasible location for an actuator. An example of an application of this general type of control system is a controller that reduces vibrations of the first mode of a cantilever beam. It is desirable to place the sensor at the tip where the largest displacement and velocity occur. However, the actuator may have to be attached near the root of the beam. It may also be desirable to sense at a translational degree of freedom and input a moment at a rotational degree of freedom or vice versa.

Since general controller schemes can lead to system designs that are dynamically unstable, stability constraints must be used during the optimization procedure. This requires the computation of the closed-loop complex eigenvalues. The more general control system scheme also leads to nonsymmetric augmented system stiffness and viscous damping matrices. The augmented system stiffness matrix $[K_A]$ is the sum of the system stiffness matrix $[K]$ and the position gain matrix $[H_p]$. The augmented system viscous damping matrix $[C_A]$ is the sum of the system viscous damping matrix $[C]$ and the velocity gain matrix $[H_v]$. The lack of symmetry in the $[K_A]$ and $[C_A]$ matrices leads to different sets of right- and left-side eigenvectors, and both sets must be calculated to carry out the eigenvalue sensitivity analysis.

Implementation of Noncollocated Controllers

In this paper a controller is defined to act in the global coordinate system with the gains assembled directly into the augmented stiffness and viscous damping matrices. A single, but separate, gain value is assembled into each of the augmented matrices. This value is added to the row of the actuator degree of freedom in the column of the sensor degree of freedom. The value that is added is positive. This choice of sign convention is logical for the case where the forcing and sensing are done on the same translational degree of freedom because it gives the same result as a constrained axial control element. In other cases involving sensing a displacement or rotation at one degree of freedom and applying a force or moment at another, the definition of positive gain is less physical, and it simply becomes a sign convention.

Dynamic Stability Constraints

Two measures of dynamic stability are the real part of the complex eigenvalue σ and the damping ratio ξ. The complex eigenvalue λ is shown in Eq. (1). The imaginary part ω_d is the damped frequency. The damping ratio is defined to be the negative of the normalized real part of the complex eigenvalue, [Eq. (2)]:

$$\lambda = \sigma + i\omega_d \tag{1}$$

$$\xi = \frac{-\sigma}{\sqrt{\sigma^2 + \omega_d^2}} \tag{2}$$

A system is dynamically stable when, for each mode, the real parts of the complex eigenvalues are negative and hence the damping ratios are positive for each mode. The stability of the higher modes may not be of interest since these modes are difficult to excite and often have low amplitudes. The real part of the complex eigenvalue is the exponential decay constant of the amplitude of vibration in the time domain while the damping ratio is the exponential decay constant of the amplitude of vibration from one cycle to the next (proportional to the logarithmic decrement for small damping). If the damping ratio is constrained to be greater than some fixed value, then the higher frequency modes will have real parts that are more negative than those of the lower frequency modes. Conversely, if all of the real parts of the complex eigenvalues are constrained to be less than some fixed value, then the higher frequency modes will have smaller damping ratios than the lower frequency modes.

If all of the damping ratios of interest are constrained to be above the same lower bound, then the higher frequency modes will tend to be more critical. It makes physical sense to constrain different modes with different damping ratios, assigning lower allowable damping ratio values to higher modes.

It is useful to include structural damping in the complex eigenvalue analysis since it tends to make the higher frequency modes have greater negative real parts. This makes sense physically since real structures show more inherent damping at higher frequencies.

Calculation of Complex Eigenvalues and Sensitivities

The equation of motion for an unloaded system is

$$[M]\{\ddot{u}\} + [C_A]\{\dot{u}\} + \left([K_A] + i\gamma[K]\right)\{u\} = \{0\} \tag{3}$$

The nonsymmetric matrix $[K_A]$ is the augmented stiffness matrix. The nonsymmetric matrix $[C_A]$ is the augmented viscous damping matrix. The factor $i\gamma[K]$ represents the structural damping of the system. By defining the state space variables as

$$\{q\} = \begin{Bmatrix} \dot{u} \\ u \end{Bmatrix} \tag{4}$$

Eq. (3) can be rewritten as

$$\begin{bmatrix} [0] & [M] \\ [M] & [C_A] \end{bmatrix}\{\dot{q}\} + \begin{bmatrix} -[M] & [0] \\ [0] & \left([K_A] + i\gamma[K]\right) \end{bmatrix}\{q\} = \{0\} \tag{5}$$

By defining

$$[M^*] = \begin{bmatrix} [0] & [M] \\ [M] & [C_A] \end{bmatrix} \tag{6}$$

and

$$[K^*] = \begin{bmatrix} -[M] & [0] \\ [0] & ([K_A] + i\gamma[K]) \end{bmatrix} \tag{7}$$

Eq. (5) can be rewritten as

$$[M^*]\{\dot{q}\} + [K^*]\{q\} = \{0\} \tag{8}$$

If harmonic solutions of the form

$$q = \{\phi\} e^{\lambda t} \tag{9}$$

are assumed, then Eq. (8) becomes

$$(\lambda[M^*] + [K^*])\{\phi\}_R = \{0\} \tag{10}$$

for the right-hand eigenvectors and

$$\{\phi\}_L^T(\lambda[M^*] + [K^*]) = \{0\}^T \tag{11}$$

for the left-hand eigenvectors. The eigenvectors are normalized so that

$$\{\phi\}_L^T[M^*]\{\phi\}_R = 1 \tag{12}$$

To facilitate efficient optimization, a first-order sensitivity analysis of the two measures of stability is needed. These sensitivities are calculated as follows.[21] The derivative of Eq. (10) is taken with respect to parameter p (which can be a structural sizing, nonstructural mass, or controller gain variable) giving

$$\lambda_{,p}[M^*]\{\phi\}_R + (\lambda[M^*]_{,p} + [K^*]_{,p})\{\phi\}_R + (\lambda[M^*] + [K^*])\{\phi\}_{R,p} = 0 \tag{13}$$

By premultiplying by $\{\phi\}_L^T$ and using Eqs. (11) and (12), Eq. (13) can be solved for $\lambda_{,p}$:

$$\lambda_{,p} = -\{\phi\}_L^T(\lambda[M^*]_{,p} + [K^*]_{,p})\{\phi\}_R \tag{14}$$

Since they are complex, $\{\phi\}$ and $[K^*]$ can be written as

$$\{\phi\} = \{\phi_r\} + i\{\phi_i\} \tag{15}$$

and

$$[K^*] = [K_r^*] + i[K_i^*] \tag{16}$$

where

$$[K_r^*] = \begin{bmatrix} -[M] & [0] \\ [0] & [K_A] \end{bmatrix} \tag{17}$$

and

$$[K_i^*] = \begin{bmatrix} [0] & [0] \\ [0] & \gamma[K] \end{bmatrix} \tag{18}$$

Substituting these and the equation for the complex eigenvalue [Eq. (1)] into Eq. (14) gives

$$\lambda_{,p} = -\{\phi_r + i\phi_i\}_L^T\left[(\sigma[M^*]_{,p} + [K_r^*]_{,p}) + i(\omega_d[M^*]_{,p} + [K_i^*]_{,p})\right]\{\phi_r + i\phi_i\}_R \tag{19}$$

The complex eigenvalue can also be broken into its real and imaginary parts [Eq. (1)]. The sensitivity of the complex eigenvalue is then

$$\lambda_{,p} = \sigma_{,p} + i\omega_{d,p} \tag{20}$$

Splitting Eq. (19) into its real and imaginary parts gives

$$\begin{aligned}\sigma_{,p} = &-\{\phi_r\}_L^T(\sigma[M^*]_{,p} + [K_r^*]_{,p})\{\phi_r\}_R \\ &+ \{\phi_r\}_L^T(\omega_d[M^*]_{,p} + [K_i^*]_{,p})\{\phi_i\}_R \\ &+ \{\phi_i\}_L^T(\sigma[M^*]_{,p} + [K_r^*]_{,p})\{\phi_i\}_R \\ &+ \{\phi_i\}_L^T(\omega_d[M^*]_{,p} + [K_i^*]_{,p})\{\phi_r\}_R\end{aligned} \tag{21}$$

which is the sensitivity of the real part (damping) and

$$\begin{aligned}\omega_{d,p} = &-\{\phi_r\}_L^T(\omega_d[M^*]_{,p} + [K_i^*]_{,p})\{\phi_r\}_R \\ &- \{\phi_r\}_L^T(\sigma[M^*]_{,p} + [K_r^*]_{,p})\{\phi_i\}_R \\ &+ \{\phi_i\}_L^T(\omega_d[M^*]_{,p} + [K_i^*]_{,p})\{\phi_i\}_R \\ &- \{\phi_i\}_L^T(\sigma[M^*]_{,p} + [K_r^*]_{,p})\{\phi_r\}_R\end{aligned} \tag{22}$$

which is the sensitivity of the imaginary part (damped frequency). The formula for the sensitivity of the damping ratio, which is formed by taking the derivative of Eq. (2) with respect to p is

$$\xi_{,p} = \frac{\omega_d(\sigma \cdot \omega_{d,p} - \omega_d \cdot \sigma_{,p})}{(\sigma^2 + \omega_d^2)^{3/2}} \tag{23}$$

Optimization Procedure

The optimization problem is stated as

$$\text{Minimize } M(\boldsymbol{p}) \tag{24}$$

or

$$\text{Minimize } \sum_i F_i(\boldsymbol{p}) \tag{25}$$

subject to behavior constraints

$$g_j(\boldsymbol{p}) \le 0, \qquad j \epsilon J \tag{26}$$

and side constraints

$$p_k^L \le p_k \le p_k^U, \qquad k \epsilon K \tag{27}$$

where M is the mass, F_i denotes the control force of controller i, $\boldsymbol{p}$ is the vector of design variables, and $g_j(\boldsymbol{p})$ represents the jth behavior constraint. The design variables can be controller gains, cross-sectional dimensions of structural elements, and nonstructural masses. The available mix of constraint options includes dynamic displacement amplitudes, controller forces, total control force, structural mass, natural frequencies, damped frequencies, damping ratios, and real parts of the complex eigenvalues.

Formulating design optimization tasks as nonlinear programming problems (NLP) is attractive because it allows simultaneous consideration of many different kinds of constraints. The primary difficulty with this approach is that direct application of nonlinear programming algorithms usually requires a large number of analyses to converge the search for an optimum point in the design space. This difficulty led to the introduction of the approximation concepts method[22] in which the original implicit NLP design problem statement is replaced by a sequence of algebraically explicit approximate design optimization problems. Each of these approximate design optimization problems can be easily solved using well-established

mathematical programming algorithms. The approximation concepts method has been found to be very effective in the context of structural synthesis and, as shown in Ref. 3, it can also be applied to the simultaneous design of a structure and its control system.

In the work reported here, the approximation concepts methods used in Ref. 3 are extended to control-augmented structural synthesis problems involving noncollocated sensor-actuator pairs and dynamic stability constraints. In each design iteration, dynamic response and real and complex eigenvalue analyses are performed to determine constraint and objective function values for the current base design. Sensitivity analysis is then carried out to evaluate gradients of the active and potentially active constraints with respect to the design variables. The gradient of the objective function with respect to the design variables is also evaluated at the current base design.

The values of the objective function and the constraints along with their gradients are used to construct an explicit optimization problem that approximates the actual synthesis problem. In this work, hybrid approximations, introduced in Ref. 23, of the form

$$g_j(p) \approx g_j(p_o) + \sum_k \frac{\partial g_j(p_o)}{\partial p_k} C_{kj} \leq 0 \tag{28}$$

where

$$C_{kj} = (p_k - p_{ok}) \quad \text{if} \quad \frac{\partial g_j(p_o)}{\partial p_k} \geq 0 \tag{29}$$

or

$$C_{kj} = -(p_{ok})^2\left[\left(\frac{1}{p_k}\right) - \left(\frac{1}{p_{ok}}\right)\right] \quad \text{if} \quad \frac{\partial g_j(p_o)}{\partial p_k} < 0 \tag{30}$$

are used. The objective function is also approximated in this manner. It should be noted that design variables that can take on negative values (e.g., position and velocity gains H_p and H_v) are treated using a shift of origin so that the foregoing approximation does not exhibit a discontinuity when various H_p or H_v pass through zero. The approximate problem is an explicit, separable, and convex inequality constrained problem that can be solved using a nonlinear inequality constrained minimization technique. The algorithm used in this work is the method of feasible directions as implemented in the CONMIN[24] optimization program. CONMIN solves the approximate problem and gives a new list of values for the design variables. These new values are used as the base point design for the next iteration. The procedure terminates on a diminishing-returns convergence criterion with respect to the objective function, namely when the relative change of the objective function values for three consecutive iterations is less than a prescribed value.

Examples

Cantilever Beam

A simple example that highlights the effects of noncollocated controllers on a structure is a cantilever beam that has controllers located at the tip and at the midspan. The thin-walled box beam is described in Fig. 1. There is a 200-kg nonstructural mass located at the center of the beam. One controller senses position and velocity at the tip and produces a force at the midspan while the other controller senses at the midspan and forces at the tip (Fig. 1). A sinusoidal force of 4000 N at 3.9 Hz is applied to the tip of the beam and the steady-state dynamic displacement of the tip is constrained to be less than 10 cm. The control force is constrained to be less than 800 N for each controller and less than 1400 N in total. The first open-loop frequency is constrained to be above 4.5 Hz. The mass of the beam is minimized subject to the above constraints. Structural sizing variables (t_1, t_2) and controller gains $(H_{p1}, H_{v1}, H_{p2}, H_{v2})$ are the design variables. Structural damping is included in the analysis.

If structural damping is not included, approximately one half of the modes will always be unstable due to the crossed controllers. About one half of the modes have displacements and velocities that are in the same direction at the tip and midspan while the others have displacements in opposite directions. This causes approximately half of the modes to become unstable when the other half are controlled. To make all the modes stable, more controllers or a different controller configuration would have to be used. The inclusion of structural damping has a more pronounced effect on the stability of the higher frequency modes. For this example, most of the results have been obtained assuming 2% structural damping.

The crossing of the controllers causes the first mode to be excited when the second is being controlled and the second to be excited when the first is being controlled. As the design is being optimized either of the modes can be the most unstable. The constraints on the stability of both modes should always be retained to avoid constraint cycling that occurs when the design changes to stabilize one mode and causes the other, unretained mode to become unstable. An iteration history of the stability constraint ($\sigma_{UB} = -0.2$ rad/s) and unconstrained designs is shown in Fig. 2.

If an upper limit is placed on the gains of the controllers, then the structure is forced to change to provide additional stability in the design. This is shown in Fig. 3. Note that large percentage changes in $-\sigma_{UB}$, the damping requirement, lead to only small increases in optimum mass.[25]

If the design is held fixed, except for the controller velocity gains, then there is a limit on the amount of stability that can be obtained for the first two modes. This is because controlling the first mode destabilizes the second. Figure 4 is a graph of the tip controller velocity gain H_{v1} plotted against the midspan controller velocity gain H_{v2}. There are two families of curves on the graph. One represents the stability of the first mode while the other represents the stability of the second mode. This graph shows that as the gains are increased, the first mode becomes more stable and the second becomes more unstable. The limit on the stability that can be attained for both modes simultaneously is $\sigma = -0.78$ rad/s.

The limit on the amount of stability that can be obtained varies with the amount of structural damping in the system. If there is no structural damping in the system, then both modes cannot be stabilized simultaneously. As structural damping is increased, the amount of attainable stability is increased. Figure 5 is a plot of the maximum attainable stability of the first two modes vs the amount of structural damping. Note that this is a linear relationship. This is because the amount of damping in each mode, assuming no controller damping, is proportional to the amount of structural damping in the system.

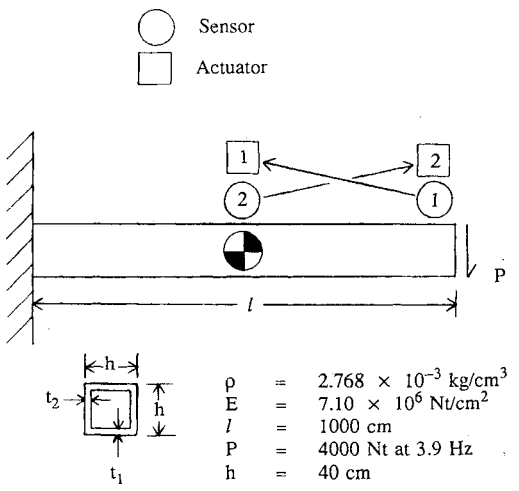

Fig. 1 Cantilever beam description.

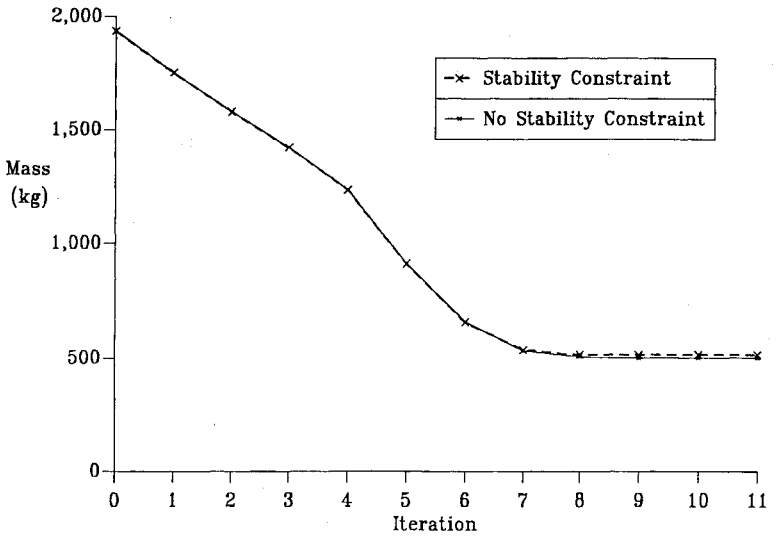

Fig. 2 Iteration history.

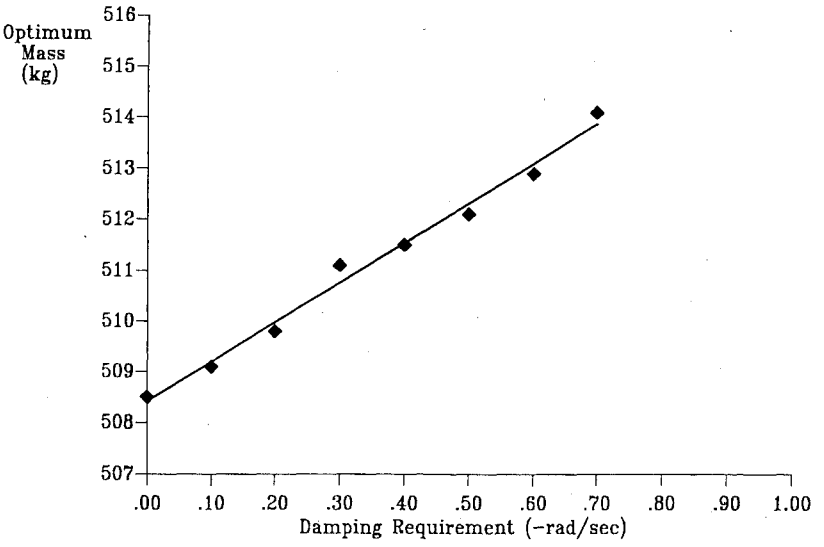

Fig. 3 Optimum mass vs damping requirement.

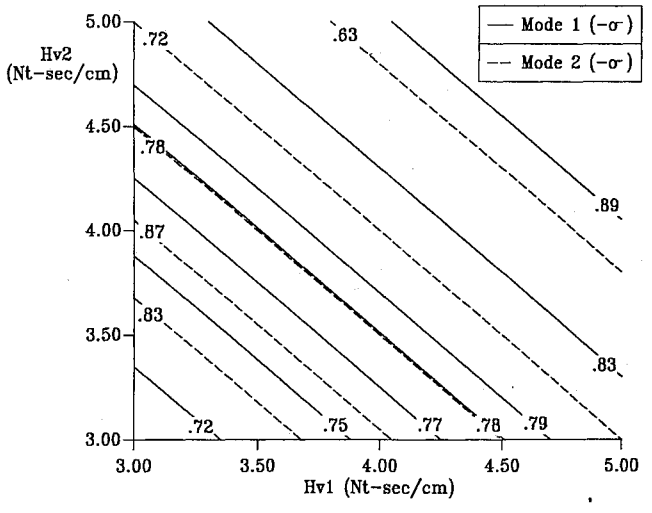

Fig. 4 Stability as a function of gain.

When there is no damping from the control system, the value of the damping ratio for every mode is twice the value of the structural damping. When damping from the control system is added, the amount of damping in each mode can change but the upper bound on the amount of the stability in the first two modes is still proportional to the structural damping value.

In this example small increases in mass of the optimized structure lead to large increases in stability, and there is an upper limit on the stability that can be obtained for the structure.

Draper/Rocket Propulsion Labororatory (RPL) Structure

The Draper/RPL structure consists of a massive central hub surrounded by four flexible appendages that have nonstructural mass attached to their free ends (see Fig. 6).[16] The entire structure is free to rotate about the central axis of the hub. Table 1 lists the important parameters. Due to symmetry, only half of the structure needs to be modeled for analysis purposes. The analysis model is shown in Fig. 7. There are four sensors on each arm at radial positions of $r = 24$ in. for sensors 2 and 6, $r = 36$ in. for sensors 3 and 7, $r = 43.6$ in. for sensors 4 and 8, and $r = 55.2$ in. for sensors 5 and 9. These sensors measure displacement and velocity in the circumferential direction. There is an additional rotational position and velocity sensor located at the axis of the hub. There are three actuators that apply torques to the structure. Actuator 1 is located at the axis of the hub, and actuators 2 and 3 are located at $r = 36$ in. on arms 1 and 2, respectively. Twenty-one controllers, with sensor-actuator pairs defined in Table 2, will be used to control the structure. The controller and actuator configuration is the

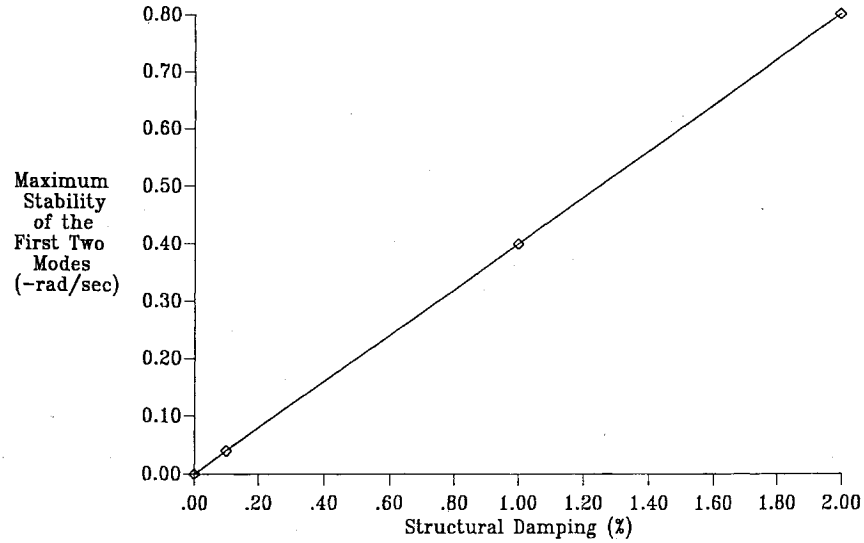

Fig. 5 Maximum stability of first two modes vs structural damping.

Table 1 Draper/RPL dimensions

Hub radius, R	12 in.
Rotary inertia of hub	1152 slug-in.^{2}
Mass density of beams	0.003021 slug/in.^{3}
Elastic modulus of arms	1.1×10^7 lb/in.^{2}
Arm thickness, t	0.125 in.
Arm height, h	6.0 in.
Arm length, l	48 in.
Tip mass	0.156941 slug
Rotary inertia of tip masses about their axis	0.2592 slug/in.^{2}
Structural damping	0.1%

Table 2 Controller sensor-actuator definitions

	Sensor								
Actuators	1	2	3	4	5	6	7	8	9
1	1	4	—	5	—	2	—	3	—
2	—	18	19	20	21	14	15	16	17
3	—	10	11	12	13	6	7	8	9

same on opposing arms. Each arm of the structure is modeled with five beam-type finite elements. The finite element nodes are located at the edge of the hub, at each sensor location, and at the tip mass.

The first nine open-loop frequencies of the structure, based on the finite element method analysis with 25 degrees of freedom, are 0.0, 0.70, 1.26, 8.18, 8.40, 24.87, 25.00, 47.65, and 47.74 Hz, respectively. The first frequency corresponds to a rigid body mode of the structure rotating about its hub axis. Note that the next eight frequencies occur in four closely spaced pairs.

Case 1

For this example the total control force, as defined in Eq. (25), is minimized subject to constraints on the closed-loop complex eigenvalues and a dynamic displacement caused by a 720 in.-lb torque at 3.0 Hz applied at the hub axis of the structure. The dynamic displacement of the tip of arm 2, and its opposing arm, are constrained to be less than 1.0 in. The damped frequency of mode one is constrained to be above 0.3 Hz, and the damping ratios for the first nine modes are constrained as follows: above 0.03 for modes 1-3, above 0.01 for modes 4-5, above 0.002 for modes 6-7, and above 0.0015 for modes 8-9.

The initial gains are $H_p = 10.0$ lb-in./rad and $H_v = 1.0$ lb-in.-s/rad for controller 1 and $H_p = 1.0$ lb and $H_v = 1.0$ lb-s for

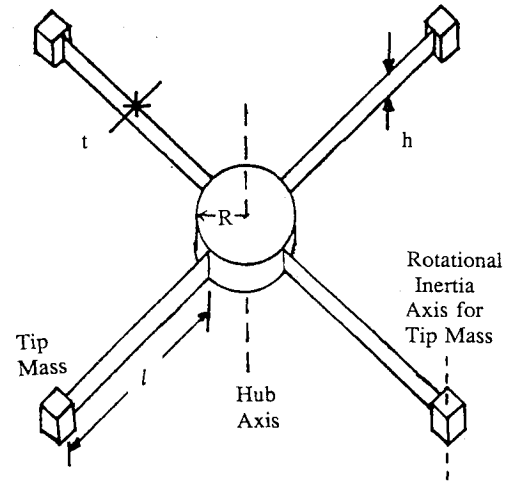

Fig. 6 Draper/RPL structure.

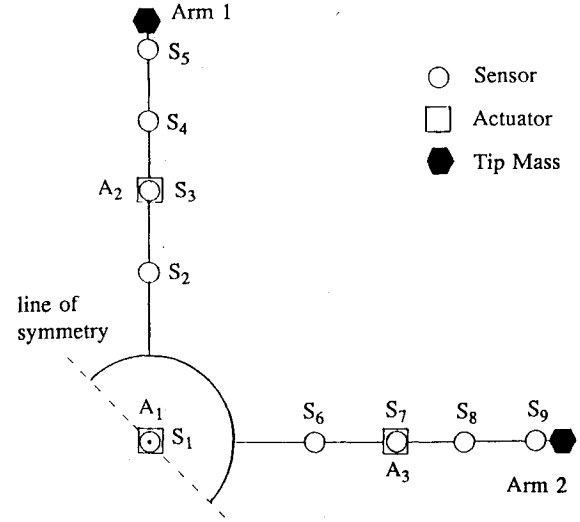

Fig. 7 Draper/RPL analysis model.

controllers 2-21. The initial and final values of the constrained parameters are shown in Table 3, and the initial and final controller torques are shown in Table 4. It is observed that the control effort has been reduced from an initial value of 214.22 in.-lb to a final value of 13.44 in.-lb and that 5 of the 11 constraints are active in the final configuration.

Table 3 Constraint parameters: effort minimization

Constraint	Constraint value	Initial value	Final value		
			Case 1	Case 2	Case 3
ξ_1	0.03	0.012	0.118	0.055	0.070
ξ_2	0.03	0.0005	0.030[a]	0.030[a]	0.030[a]
ξ_3	0.03	0.0013	0.030[a]	0.030[a]	0.030[a]
ξ_4	0.01	0.0005	0.010[a]	0.010[a]	0.010[a]
ξ_5	0.01	0.0005	0.022	0.021	0.021
ξ_6	0.002	0.0005	0.013	0.026	0.029
ξ_7	0.002	0.0005	0.068	0.044	0.044
ξ_8	0.0015	0.0005	0.0016[a]	0.0015[a]	0.0017
ξ_9	0.0015	0.0005	0.0015[a]	0.0015[a]	0.0015[a]
ω_{d_1}, Hz	0.30	0.0301	0.322	0.328	0.330
x_{Tip}, in.	b	0.133	(0.1)[b] 0.130	(0.1)[b] 0.099[a]	(0.1)[b] 0.098[a]

[a]Active constraint. [b]Values in parentheses are tip displacement limits.

Table 4 Initial and final controller torques

Controller	Initial	Final			
		Case 1	Case 2	Case 3	Case 4
1	0.48	0.23	0.15	0.22	0.46
2	8.25	0.06	0.03	0.01	0.58
3	4.50	0.35	0.01	0.05	2.50
4	8.24	0.01	0.03	0.01	0.20
5	4.50	0.00	0.01	0.00	2.45
6	8.25	1.08	1.75	2.24	1.21
7	7.54	0.20	2.37	2.43	1.01
8	4.50	2.62	3.02	2.42	1.42
9	0.00	0.06	0.26	0.25	0.92
10	8.24	0.02	0.12	0.05	2.47
11	7.54	0.01	0.07	0.11	2.48
12	4.50	0.00	0.06	0.09	2.34
13	0.00	0.01	0.01	0.03	2.50
14	8.25	0.30	0.04	0.22	1.11
15	7.54	0.57	0.02	0.34	1.80
16	4.50	0.54	0.03	0.30	0.84
17	0.00	0.07	0.26	0.41	2.47
18	8.24	0.25	0.02	0.00	0.13
19	7.54	0.01	0.02	0.00	2.28
20	4.50	0.33	1.13	1.29	0.15
21	0.00	0.00	0.00	0.01	0.73
Total controller force (in.-lb)	214.22	13.44	18.82	20.96	60.10

Table 5 Gains for case 3

Controller	H_p (lb[a])	H_v (lb/s[b])
1	9.625	0.123
2	−0.001	0.001
3	0.218	−0.001
4	0.032	0.000
5	0.005	0.001
6	4.541	−0.124
7	5.935	0.091
8	9.017	0.263
9	3.205	0.639
10	−0.104	0.003
11	−0.274	0.003
12	−0.350	0.007
13	−0.015	0.272
14	0.499	−0.004
15	0.842	−0.009
16	1.241	−0.016
17	1.506	1.110
18	−0.001	−0.001
19	−0.001	0.000
20	0.002	−0.290
21	0.357	0.126

[a]Except controller 1, which is in.-lb/rad.
[b]Except controller 1, which is in.-lb-s/rad.

Table 6 Constraint parameters: mass minimization

Constraint	Constraint value	Initial value	Final value
ξ_1	0.030	0.012	0.051
ξ_2	0.030	0.0015	0.032
ξ_3	0.030	0.0023	0.030[a]
ξ_4	0.010	0.0015	0.014
ξ_5	0.010	0.0015	0.012
ξ_6	0.002	0.0015	0.0027
ξ_7	0.002	0.0015	0.0471
ξ_8	0.0015	0.0015	0.0026
ξ_9	0.0015	0.0013	0.0015[a]
ω_{d1}, Hz	0.0477	0.0387	0.1615
ω_{d2}, Hz	0.7161	0.6958	0.7161[a]
ω_{d3}, Hz	1.321	1.260	1.321[a]
$x_{\text{Tip 1}}$, in.	0.1	0.133	0.099[a]
$x_{\text{Tip 2}}$, in.	0.1	0.133	0.097[a]
Control force (in.-lb)	60.0	570.1	60.1[a]

[a]Active constraint.

Case 2

This is the same as case 1 except that the tip displacement of arm 2 has now been constrained to be less than 0.1 in. This causes a 40% increase in the amount of controller force needed to satisfy the constraints. Controllers 6, 7, 8, and 20 exhibit the largest increases in control effort (see Table 4).

Case 3

This is the same as case 2 except that the control effort of each controller has been limited to 2.5 in.-lb. This causes a 10% increase in total control effort. The final gain values for this case are shown in Table 5.

In summary, these first three cases show that tighter constraints on dynamic displacements lead to an increase in control force and that an upper bound on individual controller force causes an increase in total control force. As one would expect, the tip displacement and several damping ratio constraints become active as the total control force is minimized.

Case 4: Mass Minimization

In this case the mass of the structure will be the objective function to be minimized. The thickness of the 10 beam elements and 2 tip masses will be included with the controller gains as design variables. The dynamic displacements of the tips of both arms are constrained to be less than 0.1 in. The previous damping ratio constraints and lower-bound constraints on the first three damped frequencies of 0.0477, 0.7162, and 1.321 Hz, respectively, are also included. The total control effort is constrained to be less than 60.0 in.-lb. These constraints are summarized in Table 6. The maximum allowable torque for any single controller is constrained to be below 2.5 in.-lb. The structural damping for this case is 0.3%. In this example 54 design variables and 36 constraints are considered.

Table 7 Initial and final structural parameters

		Parameter	Initial	Final
Arm 1	Hub	t_1 in.	0.1250	0.1005
		t_2	0.1250	0.1066
		t_3	0.1250	0.1142
		t_4	0.1250	0.1087
	Tip	t_5	0.1250	0.1198
Arm 2	Hub	t_6 in.	0.1250	0.1009
		t_7	0.1250	0.1025
		t_8	0.1250	0.1117
		t_9	0.1250	0.1056
	Tip	t_{10}	0.1250	0.1092
		M_1 (slug)	0.156941	0.1200[a]
		I_1 (slug-in.^{2})	0.2592	0.2664
		M_2 (slug)	0.156941	0.1200[a]
		I_2 (slug-in.^{2})	0.2592	0.2592
		Mass	1.063	0.852

[a] At lower bound.

Convergence of 0.1% is achieved in 24 iterations. The initial and final structural parameters are shown in Table 7, and the initial and final constraint values are shown in Table 6. Controllers 3, 5, 10, 11, 13, and 17 have control torques that are at the upper limit (see Table 4).

This case shows that the mass of a structure can be effectively minimized while the control system gains are simultaneously being changed to satisfy complex eigenvalue and harmonic dynamic displacement constraints.

Conclusions

The characteristics of a noncollocated control system must be kept in mind when trying to simultaneously synthesize a structure and its control system. Since controllability is not guaranteed, it may not be possible to achieve the required amount of damping in a structure with a given controller configuration. It is helpful to include the structure's inherent damping, if it can be conservatively characterized, in the analysis as it will tend to stabilize the higher frequency modes. Since these modes are harder to control, when only a limited number of actuators can be used, the inclusion of inherent damping is desirable.

The dynamic stability of a structure can be very sensitive to its mass. This suggests that further work should be done to examine the robustness of a control system that has been synthesized while the mass of the structure is being minimized.

The last example (case 4) shows that this extension of the control-augmented structural synthesis approach can effectively handle a diverse mix of constraints including closed-loop eigenvalues, direct limits on controller forces, total control force, and specific response quantities (e.g., peak displacements at prespecified locations). Natural frequency as well as static stress and displacement constraints can also be included. This work shows that the approximation concepts approach can be extended to efficiently solve control-augmented structural synthesis problems that require inclusion of dynamic stability constraints.

Acknowledgments

This research was supported by NASA Research Grant No. NSG-1490. The authors would like to thank R. V. Lust of the General Motors Research Laboratories for his helpful advice and unending patience during this work.

References

[1]Garibotti, J. F., "Requirements and Issues for the Control of Flexible Space Structures," *Proceedings of the AIAA/ASME/ASCE/AHS 25th Structures, Structural Dynamics, and Materials Conference,* AIAA, Washington, DC, 1984, pp. 338–347.

[2]Pinson, L. D., Amos, A. K., and Venkayya, V. B. (eds.), "Modeling, Analysis and Optimization Issues for Large Space Structures," *Proceedings of a NASA/AFOSR Workshop,* NASA, Washington, DC, 1982.

[3]Lust, R. V., and Schmit, L. A., "Control-Augmented Structural Synthesis," *AIAA Journal,* Vol. 26, No. 1, 1988, pp. 86–94.

[4]Lust, R. V., and Schmit, L. A., "Control Augmented Structural Synthesis," NASA CR-4132, April 1988.

[5]Hale, A. L., Lisowski, R. J., and Dahl, W. E., "Optimal Simultaneous Structural and Control Design of Maneuvering Flexible Spacecraft," *Journal of Guidance, Control, and Dynamics,* Vol. 8, No. 1, 1985, pp. 86–93.

[6]Cha, J. Z., Pitarresi, J. M., and Soong, T. T., "Optimal Design Procedures for Active Structures," *Journal of Structural Engineering,* Vol. 114, No. 12, 1988, pp. 2710–2723.

[7]Miller, D. F., Venkayya, V. B., and Tischler, V. A., "Integration of Structures and Controls—Some Computational Issues," *Proceedings of the 24th Conference on Decision and Control,* IEEE, New York, Dec. 1985, pp. 924–931.

[8]Onoda, J., and Haftka, R. T., "An Approach to Structure/Control Simultaneous Optimization for Large Flexible Spacecraft," *AIAA Journal,* Vol. 25, No. 8, 1987, pp. 1133–1138.

[9]Belvin, W. K., and Park, K. C., "Structural Tailoring and Feedback Control Synthesis: An Interdisciplinary Approach," *Proceedings of the AIAA/ASME/ASCE/AHS 29th Structures, Structural Dynamics, and Materials Conference,* AIAA, Washington, DC, April 1988, pp. 1–8.

[10]Miller, D. F., and Shim, J., "Gradient Based Combined Structural and Control Optimzation," *Journal of Guidance, Control, and Dynamics,* Vol. 10, No. 3, 1987, pp. 291–298.

[11]Khot, N. S., Venkayya, V. B., and Eastep, F. E., "Optimal Structural Modifications to Enhance the Active Vibration Control of Flexible Structures," *AIAA Journal,* Vol. 24, No. 8, 1986, pp. 1368–1374.

[12]Becus, G. A., Lui, C. Y., Venkayya, V. B., and Tischler, V. A., "Simultaneous Structural and Control Optimization via Linear Quadratic Regulator Eigenstructure Assignment," *Proceedings of the 58th Shock and Vibration Symposium,* NASA, Washington, DC 1987.

[13]Junkins, J. L., and Rew, D. W., "A Simultaneous Structure/Controller Design Iteration Method," *Proceedings of the 4th American Control Conference,* IEEE, New York, 1985.

[14]Messac, A., Turner, J., and Soosaar, K., "An Integrated Control and Minimum Mass Structural Optimization Algorithm for Large Space Structures," *Proceedings of the Workshop on Identification and Control of Large Space Structures,* Jet Propulsion Laboratory (JPL) Publication 85-29, Pasadena, CA, April 1985, pp. 231–266.

[15]Hale, A. L., "Integrated Structural/Control Synthesis via Set-Theoretic Methods," *Proceedings of the AIAA/ASME/ASCE/AHS 26th Structures, Structural Dynamics, and Materials Conference,* AIAA, Washington, DC, April 1985, pp. 636–641.

[16]Bodden, D. S., and Junkins, J. L., "Eigenvalue Optimization Algorithms for Structure/Controller Design Iterations," *Journal of Guidance, Control, and Dynamics,* Vol. 8, No. 6, 1985, pp. 697–706.

[17]Messac, A., and Turner, J., "Dual Structural-Control Optimization of Large Space Structures," AIAA Paper 84-1044-CP, May 1984.

[18]Knot, N. S., Öz, H., Grandhi, R. V., Eastep, F. E., and Venkayya, V. B., "Optimal Structural Design With Control Gain Norm Constraint," *AIAA Journal,* Vol. 26, No. 5, 1988, pp. 604–611.

[19]Adamian, A., and Gibson, J. S., "Integrated Control/Structure Design and Robustness," SAE Transactions Aerospace, Warrendale, PA, Vol. 95, Section 7, 1986, pp. 1336–1343.

[20]Onoda, J., and Watanabe, N., "Integrated Direct Optimization of Structure/Regulator/Observer for Large Flexible Spacecraft," *Proceedings of the AIAA/ASME/ASCE/AHS/ASE 30th Structures, Structural Dynamics, and Materials Conference,* AIAA, Washington, DC, April 1989, pp. 1336–1344.

[21]Plaut, R. H., and Huseyin, K., "Derivatives of Eigenvalues and Eigenvectors in Non-Self-Adjoint Systems," *AIAA Journal,* Vol. 11, No. 2, 1973, pp. 250–251.

[22]Schmit, L. A., and Miura, H., "Approximation Concepts for Efficient Structural Synthesis," NASA CR 2552, March 1976.

[23]Starnes, J. R., Jr., and Haftka, R. T., "Preliminary Design of Composite Wings for Buckling, Stress and Displacement Constraints," *Journal of Aircraft,* Vol. 16, No. 8, 1979, pp. 564–570.

[24]Vanderplaats, G. N., "CONMIN—A Fortran Program for Constrained Function Minimization," NASA TM X-62,682, Aug. 1973.

[25]Haftka, R. T., Martinovic, Z. N., Hallauer, W. L., Jr., and Schamel, G., "Sensitivity of Optimized Control Systems to Minor Structural Modifications," *Proceedings of AIAA/ASME/ASCE/AHS 26th Structures, Structural Dynamics, and Materials Conference,* AIAA, Washington, DC, April 1985, pp. 642–650.